Chin. J. Chem. Eng., **15**(6) 821—827 (2007)

Experimental Investigation of Single-phase Flow in Structured Packing by LDV*

CHEN Jiangbo(陈江波)**, LIU Chunjiang**(刘春江)**, **LI Yingke**(李莹珂)**, HUANG Ying**(黄莹)**,**
YUAN Xigang(袁希钢) **and YU Guocong**(余国琮)
State Key Laboratory of Chemical Engineering, Chemical Engineering Research Center, Tianjin University, Tianjin 300072, China

Abstract To date, many models have been developed to calculate the flow field in the structured packing by the computational fluid dynamics (CFD) technique, but little experimental work has been carried out to serve the validation of flow simulation. In this work, the velocity profiles of single-phase flow in structured packing are measured at the Reynolds numbers of 20.0, 55.7 and 520.1, using the laser Doppler velocimetry (LDV). The time-averaged and instantaneous velocities of three components are obtained simultaneously. The CFD simulation is also carried out to numerically predict the velocity distribution within the structured packing. Comparison shows that the flow pattern, velocity distribution and turbulent kinetic energy (for turbulent flow) on the horizontal plane predicted by CFD simulation are in good agreement with the LDV measured data. The values of the *x*-and *z*-velocity components are quantitatively well predicted over the plane in the center of the packing, but the predicted *y*-component is significantly smaller than the experimental data. It can be concluded that experimental measurement is important for further improvement of CFD model.
Keywords velocity profile, structured packing, laser Doppler velocimetry, computational fluid dynamics

1 INTRODUCTION

Structured packing is widely used in chemical and biochemical industries as static mixer or distillation column internals. The hydrodynamic behavior of the fluids is of great importance in determining the process performance involved with structured packing[1]. Up still, many numerical investigations have been carried out to simulate the flow field in the structured packing by the computational fluid dynamics (CFD) technique, but most of them were validated by pressure drop or other macro scale experiment. Detailed information about the flow field by experiment for structured packing is still lacking in the literature.

Among the theoretical investigations on the flow behavior in structured packing, Hodson *et al*.[2] may be the first which using CFD method to simulate the flow pattern of the vapor phase on the micro-scale within the channels of the structured packing. Van Gulijk[3] presented a simplified model, the "Toblerone" model, to investigate the transversal dispersion behavior with the CFD code, CFX. Based on van Gulijk's work, Higler *et al*.[4] and van Baten *et al*.[5,6] studied the liquid phase mixing and mass transfer within a catalytic packed-bed reactor which contained Katapak-S structure. Petre and Larachi[7,8] considered the structured packing layers as the combination of four representative elementary units (REU), simulated the aerodynamics in each REU using three-dimensional CFD and reconstructed the overall pressure drop in single gas-phase flow in structured packing. Using the volume-averaging method, Zhang *et al*.[9] proposed a CFD model to describe the liquid flow behavior in a structured packing column without taking the gas-phase behavior into account.

For simulating two-phase flow within a structured packed bed, Szulczewska *et al*.[10] built a two-dimensional model to calculate the gas-liquid interfacial area and study the mechanism of droplet formation and liquid film breaking during gas-liquid countercurrent flow over the vertical flat and corrugated plate. Li *et al*.[11] numerically simulated the droplet behavior in the wave-type flow channel, and the predicted pressure drop and separating efficiency are in good agreement with the air-water experimental results. Gu *et al*.[12] presented a two-phase model, based on the volume of fluid (VOF) method to predict the hydrodynamics of falling film flow over the corrugated plate and interpret the effects of the plate surface microstructure, liquid properties and gas-liquid interaction. Also *via* the VOF approach, Raynal *et al*.[13] successfully estimated the liquid film thickness and thus the liquid holdup in structured packing (a two-dimensional zigzag channel). Valluri *et al*.[14,15], using a CFX code, simulated flow of water over the doubly sinusoidal surface of Mellapak 500Y at $Re=10.45$ and 200, and found that there exists re-circulation regions in the substrate 'valleys' at the Reynolds number of 200.

Additionally, it was noted that all the works mentioned above used pressure drop or liquid holdup to validate their theoretical models. To the authors' knowledge, there is still no published experimental report on measuring the velocity distribution within the structured packing, even for single-phase flow, due to its complex geometry and the lack of an effective measuring tool. For two-phase flow in the structured packing, it is much harder to measure the velocity profiles, because of the difficulty of determining the free surface of liquid phase.

Received 2007-01-30, accepted 2007-09-24.
* Supported by the National Natural Science Foundation of China (No.20476072).
** To whom correspondence should be addressed. E-mail: cjliu@tju.edu.cn

For investigating the detailed information of complex flow, laser Doppler velocimetry (LDV)[16,17], particle image velocimetry (PIV)[18,19], and magnetic resonance imaging (MRI)[20] were commonly used techniques. In this work, LDV was used to measure the velocity profile within the structured packings. However, as pointed out by Gunjal *et al*.[21], it is difficult to experimentally study the influence of all key parameters. Here, the single-phase flow through the structured packing was also simulated using computational fluid dynamics. The CFD simulations were carried out in a 3-dimensional geometry which corresponded to the domain within two adjacent corrugated plates. The simulated velocity distribution was compared with the experimental measurements. The model and results discussed here may be helpful for the understanding of the flow within structured packed beds.

2 EXPERIMENTAL SETUP AND MEASUREMENT SCHEME

A schematic diagram of the experimental system is shown in Fig.1, including (a) a photograph of experimental setup and (b) the scheme of experimental flow sheet. The setup mainly consisted of two adjacent corrugated plates, the liquid circulation system, and the LDV system.

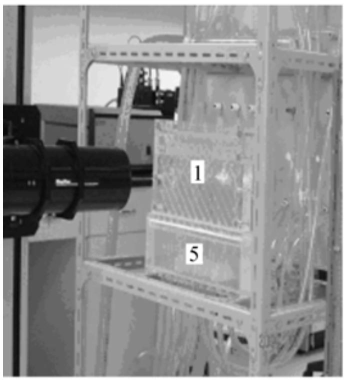

(a) Experiment apparatus

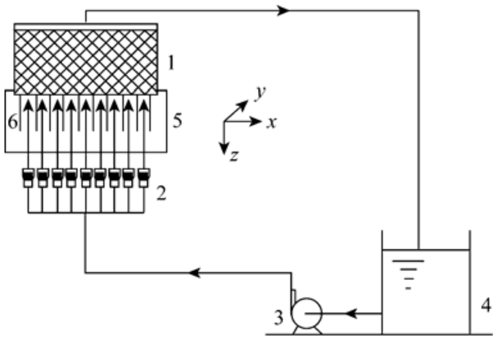

(b) Experimental flow sheet

Figure 1 The schematic diagram of the experimental system

1—Plexiglas packing; 2—rotameter; 3—centrifugal pump; 4—liquid tank; 5—liquid distributor; 6—partitioning plate

The measuring box was composed of two pieces of Plexiglas corrugated plates. The front plate inclined to the left while the back one to the right. The size of each plate was 312mm×190mm×20mm. The corrugation crest height and corrugation base length of the plate were 10mm and 29.3mm, respectively, and corrugations inclined at 45° with respect to the horizontal. The hydraulic diameter of the flow channel is $d_{\mathrm{h}}=0.033\mathrm{m}$. The space embraced by two plates was the domain of measurement. The measurement was made at atmospheric pressure and room temperature. Glycerol aqueous solution (65%, mass fraction), with a density of $1167\mathrm{kg\cdot m^{-3}}$, a dynamic viscosity of 0.01554Pa·s, and a refractive index of 1.42[22], was selected as the test liquid to minimize the refractive effect of Plexiglas, with a refractive index of 1.48.

As shown in Fig.1, the liquid circulation system comprised a centrifugal pump, a set of liquid distributor and nine rotameters. The liquid distributor was practically a cuboid box, in which there were ten partitioning plates evenly distributed inside the box to obtain an even flow profile at its outlet. The glycerol aqueous solution was pumped from the tank, flowing through nine transparent pipes and entered the liquid distributor. The pipes were evenly distributed at the entrance of the distributor. At each pipe, a rotameter with measuring range of $6—60\mathrm{L\cdot h^{-1}}$ was used to control the flow rate. The overflow liquid atop the packing was circulated to the tank. To avoid air entering into the packing during the experiment, the liquid was introduced from the bottom.

A Dantec 3D Fiberflow LDV system was used to measure the liquid velocity profile inside the packing. The system consisted of a 5 W argon ion laser emitter (Spectra-Physics-Laser, 2017), transmitting and receiving optics, a signal processor (57N20 BSA), a traversing system and a control computer. In the experiment, the glycerol aqueous solution was seeded with hollow glass particles with the diameter of 8—12μm and a density of $1360\mathrm{kg\cdot m^{-3}}$ (the volume fraction of the particles about 10^{-4}). A lens with a focal length of 310mm was mounted on the LDV probe. A frequency shift of 40MHz was used to remove the directional ambiguity of the velocity. Three colored beams (purple, green and blue) was actually used for measurements. The signals were processed by BSA processor, connected to a computer, and then converted into transient velocity values by the BSA flow v2.1 software package[23]. By statistical analysis, the time-averaged velocity and fluctuated velocity were obtained.

In the experiments, the velocity distributions were measured at the horizontal plane of the packing in detail for the Reynolds number of 20.0, 55.7 and 520.1. To avoid the influence of the outlet effect, the measurement of x and z velocity components was made in three selected regions of the horizontal plane, 88mm below from the outlet of the structured packing, as shown in Fig.2. On each plate, the distance between the stagger crests of two packings was 10mm. The width of each region was set about two times corrugation base length, 58mm. The right, central and left measuring regions in the plane was 12mm, 114mm and 224mm away from the right side of the packing, respectively.

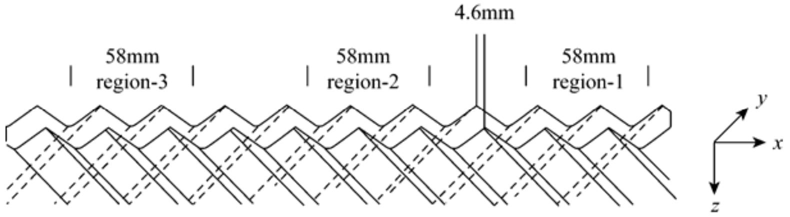

Figure 2 The measured regions in the horizontal measurement plane

Besides, to determine the flow parameters of the liquid, the turbulent kinetic energies, calculated by Eq.(1), at a typical point in the center of the plane were obtained at different Reynolds numbers:

$$k = \frac{1}{2}\sum_{i=1}^{3}\left(\overline{u_i^2} - \bar{u}_i^2\right) \quad (1)$$

where u_i is the instantaneous velocity component and $\bar{u}_i$ is the average over all velocity samples. In the measurements, the 3D non-coincidence mode was taken to measure the three velocity components. For each measured region, a 2mm×1mm mesh was plotted in its x—y cross section. Generally, the sampling frequency is about 200—3400Hz at the center of the channel, and 10—50Hz near the wall. At each point, the sampling time was 20s, determined by the repetitive experiments.

3 NUMERICAL SIMULATION

The commercial CFD software package, Fluent v6.1, was used to predict the velocity profile inside the packing which was exactly the same as those used in the LDV measurements. For turbulent flow, the turbulent viscosity was calculated by the renormalized group (RNG) $k-\varepsilon$ model. Since the concentration of the added particle was dilute, the interactions due to particles were negligible. In the simulation, the fluid was considered to be incompressible and isothermal, and thus the liquid properties were constant. The computational domain of the model was shown in Fig.3. Considering its complex geometry, the non-structured tetrahedral grid was used in the simulation.

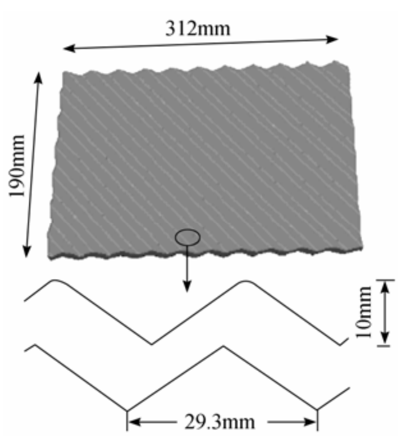

Figure 3 Computational domain of the model

The mathematical model describing the flow included the mass and momentum conservation equations, and the $k-\varepsilon$ model may be referred to the Fluent User's Guide[24] for more details of the mathematic model.

The boundary conditions used are as follows: (1) at the liquid inlet, a constant velocity was specified, and the flow direction was defined normal to the boundary; (2) at the outlet, the flow is considered to be fully developed, that is, the diffusion flux for all flow variables in the exit direction are zero; (3) non-slip condition was used at the walls, and the flow behavior in the region near the walls was approximated using the "standard wall functions."

The finite-volume method was employed to solve the partial differential equations, using a segregated numerical scheme with implicit linearization. The pressure values were interpolated on the faces using momentum equation coefficients and the SIMPLE pressure-velocity coupling algorithm.

For investigating the grid dependence of the solution, four different computational grids (consisting of 57542, 169984, 284834 and 448326 cells, respectively) were generated. The numerical experiments were carried out with the first-order upwind discretization scheme. As shown in Fig.4, the simulated pressure drops were plotted against the number of cells. It was found that 169984 cells were enough for the calculation.

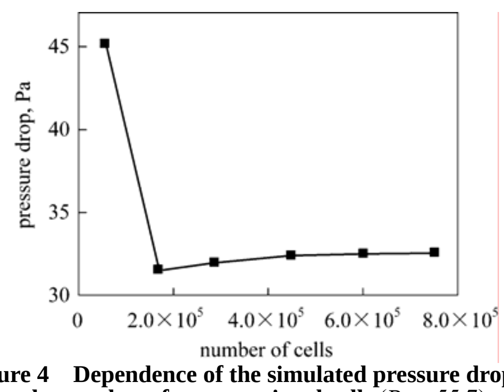

Figure 4 Dependence of the simulated pressure drop on the number of computational cells (Re=55.7)

In the simulation, the under-relaxation factor for pressure was set to 0.1 at the beginning and was increased up to 0.3 as the solution progressed. The under-relaxation factor for momentum was set to 0.2. When the residuals fell below 1×10^{-3} for all equations, the simulation was considered converged.

4 RESULTS AND DISCUSSION

The velocity profiles were measured at three Reynolds numbers of 20.0, 55.7 and 260.1, and the CFD simulations were conducted at exactly the same conditions. Before the calculation, the nature of liquid flow was determined by the experiment. Fig.5 presented the relation between the turbulent kinetic energy and the Reynolds number, showing that, when the Reynolds number is lower than 200, the turbulent kinetic energy increases slightly with *Re*, which indicates the flow is laminar; when *Re* rises up to 300, the turbulent kinetic energy increases greatly, and the flow has developed to be transitional. When the Reynolds number increases higher than 300, the turbulent kinetic energy increases rapidly, which means that the fluid has become turbulent. Referring to this observation, it can be concluded that the flows at the Reynolds numbers of 20.0 and 55.7 are laminar, and at the Reynolds number of 520.1, the flow is turbulent in the simulation.

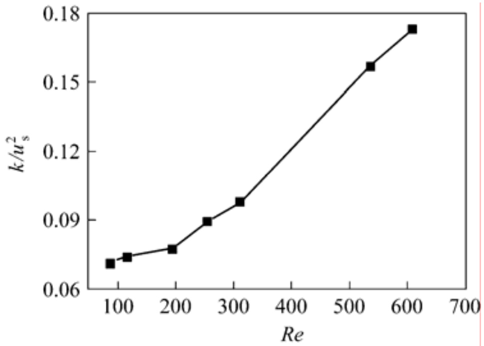

Figure 5 Relation between the turbulent kinetic energy and the Reynolds number from experiment

In the following discussion, the LDV-measured velocities are time-averaged measurements.

4.1 Flow patterns

In this part, the flow patterns in a horizontal cross section within the structured packing were discussed qualitatively. First of all, it should be pointed out that the measured flow patterns in the different regions on the same plane are very similar, which will be validated in the latter part of this paper. And as a result, only the results in one measurement region are provided here.

Figure 6 illustrated the experimental results in the region-2 compared with CFD predicted ones in the form of vectors which composed of *x*- and *y*- velocities. The Reynolds number of the flow is 55.7. From experimental results in these figures, it could be found that the horizontal flow patterns show certain similarities to a certain extent, in different regions of the same plane. Generally, the fluid flowed around the valleys of the packing opposite to the projection of the inclining direction of the triangular channel. It can be observed from Fig.6(a) that, under the influence of the structure of the packing, there exist obvious circulation areas in the region. The typical circulation area appears in the center of the wider channel.

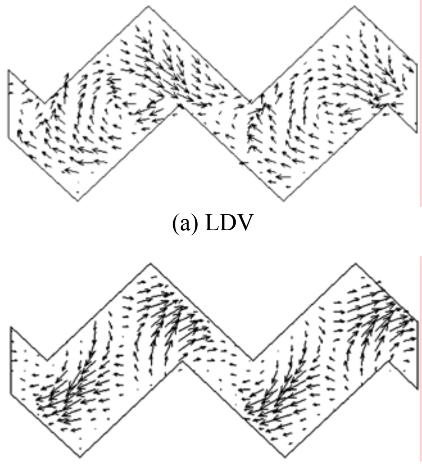

(a) LDV

(b) CFD

Figure 6 Flow pattern comparison in region-2 in the measurement plane (Re=55.7)

Figure 6(b) presents the CFD predicted flow pattern in the region, corresponding to the region-2 in the experiment. By comparison, it can be seen that the flow pattern of the experimental and computational result is roughly the same, but the experimental map shows a little more complexity than the CFD calculated one. In the center of the wider channel, the circulation area is reproduced by the simulation, but not so obviously.

Due to the similar reason as mentioned above, only the results in the region-2 of the plane at the Reynolds number of 20.0 and 520.1 are given in Figs.7 and 8, respectively. Comparing Fig.7(a) with Fig.6(a), it can be found that the flow patterns at the Reynolds numbers of 20.0 and 55.7 are very similar, except that the circulation area is smaller at lower Reynolds number. At the Reynolds number of 520.1, however, the circulation area is not as obviously observable as that at the Reynolds numbers of 20.0 and 55.7. The reason may be that the flow has developed to be turbulent and the flow field is not greatly affected by the structure of the packing. The CFD calculated results at the Reynolds numbers of 20.0 and 520.1 also approximately reproduced those measured in the experiment.

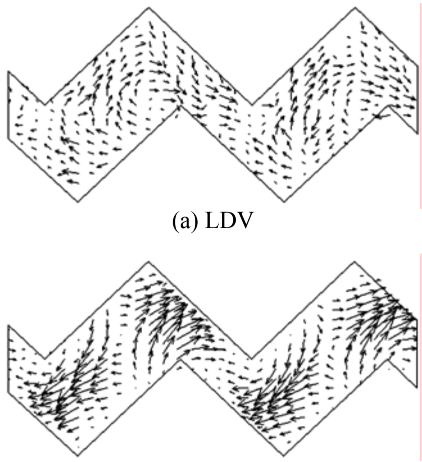

(a) LDV

(b) CFD

Figure 7 Horizontal flow pattern comparison in region-2 in the plane (Re=20.0)

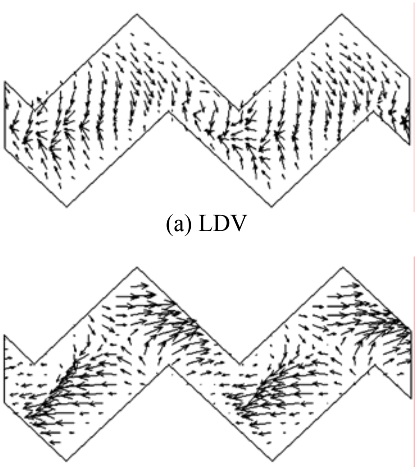

(a) LDV

(b) CFD

Figure 8 Horizontal flow pattern comparison in region-2 in the plane (Re=520.1)

4.2 Vertical velocity component

Figure 9 gave the distributions of z-velocity in three regions obtained by the LDV measurements at the Reynolds number of 55.7. From the figure, it could be found that the distributions of z-velocity in the region-1 and region-2 are well in agreement, but a little different from that in the region-3. Even so, it could be concluded that, in some extent, the liquid entered the packing uniformly. Comparing the velocity distribution profiles of z-velocity in different regions, it can be also found that the values in the center of the channel are relatively higher, and the maximum values of z-velocity are about $0.07 \mathrm{m \cdot s^{-1}}$.

Figure 10 presented the distribution of z-velocity obtained by CFD simulation in the region-2. Comparing with LDV measured results, it can be seen that both the distribution structure and the range of z-velocity are in good agreement.

The z-velocity distributions measured by the LDV measurements at the Reynolds numbers of 20.0 and 520.1 showed the similar characters as those at the Reynolds numbers of 55.7, and hence, the figures are not given here.

4.3 Quantitative comparison of CFD results with LDV data

Since the velocity distributions on the same plane are similar, and for the convenience of simplicity, the quantitative comparison is only conducted at one third of the points in the region-2. The comparison for Re=55.7 is shown in the Fig.11 (the x and y positions in the figure are relative coordinate). The velocities from the CFD simulation are collected at the same coordinate points as the LDV measurements. From the figures, it can be observed that, at most points, the x- and z-velocities are well predicted by the CFD calculations. In the center of the plane, both x- and z-velocity are higher in value. The z-velocity is slightly under-predicted by the CFD simulation. The maximum discrepancy of the z-velocity between the prediction and measurement is about 44% at x=16mm at the Reynolds number of 55.7. For x-velocity, the maximum prediction error is about 38.7% at x=52mm. At other positions, the relative prediction errors are often lower than 15%. Detailed data for other Reynolds numbers may be available from the communication to the corresponding author.

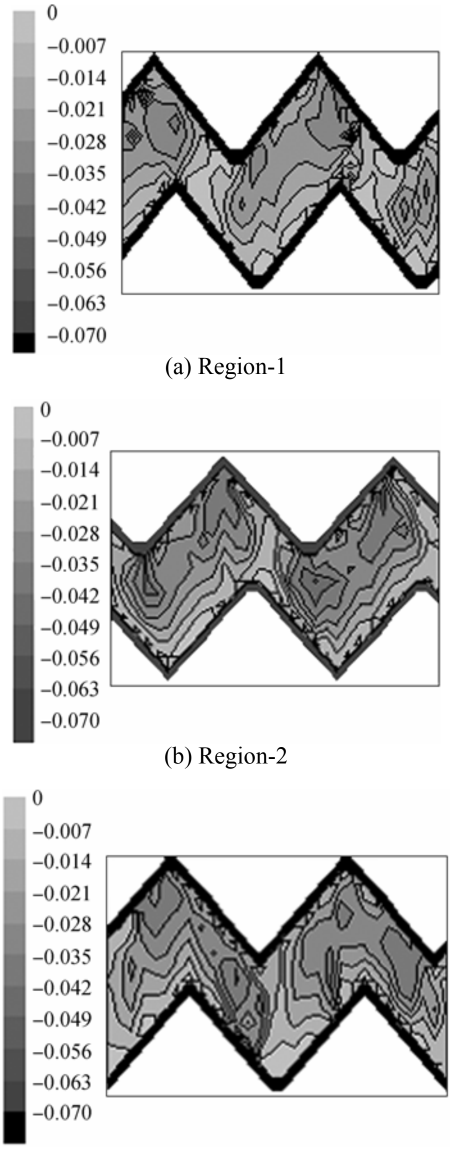

(a) Region-1

(b) Region-2

(c) Region-3

Figure 9 Contours of measured mean z-velocity in three regions of the plane (Re=55.7)

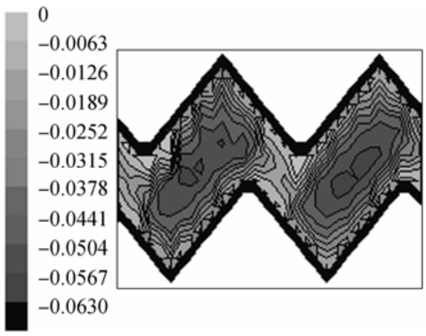

Figure 10 Contours of CFD predicted mean z-velocity in region-2 (Re=55.7)

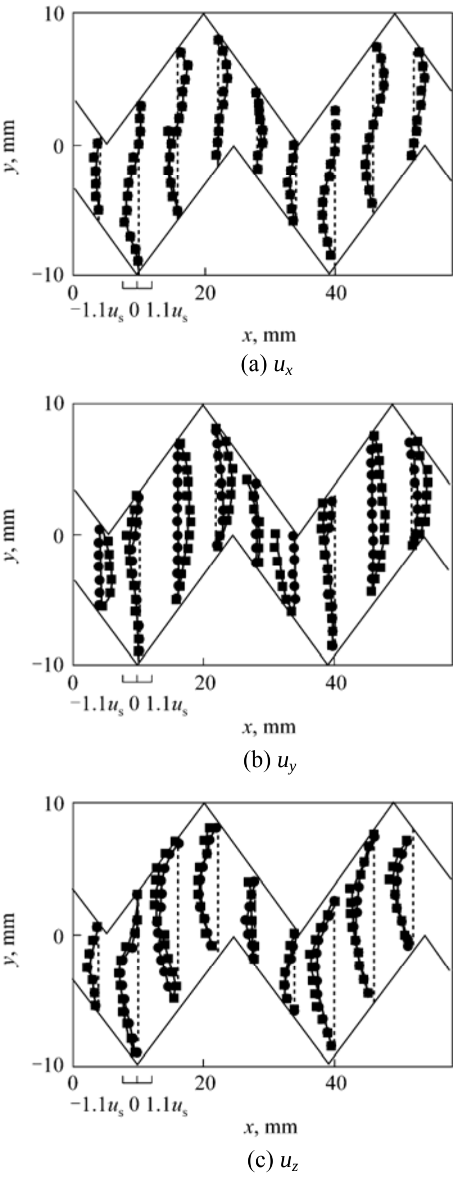

Figure 11 Mean velocity comparison in region 2 of the plane (Re＝55.7)
■ LDV; ● CFD

Unlike *x*- and *z*-velocities, *y*-velocity is under-predicted greatly compared with the experimental data for the reason mentioned above, which is the reason why the predicted flow pattern in the horizontal plane shows a little difference from the experimental result. Similar result has been found by Harris *et al*.[25], Ng *et al*.[26] and Li *et al*.[27], that the tangential velocity component was greatly under-predicted in the simulations of the flow in a stirred vessel using commercial software. These authors all attributed the results to the turbulence model used. In the current case, it can be considered that the great discrepancy of y-velocity component is caused by the same reason. Even so, the whole flow pattern on the horizontal plane is still similar.

5 CONCLUSIONS

In this work, detailed LDV measurements of the flow profile of glycerol solution in the structured packing have been carried out at the Reynolds numbers of 20.0, 55.7 and 520.1. The measured results indicate that the flow pattern in the horizontal plane the velocity distribution show good spatial periodicity. In the wider part of the flow channels, the circulation areas can be clearly observed. All three velocity components reach their maximum at the center of the packing "valley".

On the basis of the experimental observation, the CFD simulations under the same conditions are conducted. The CFD-predicted and LDV-measured values for *x*- and *z*-velocity are found to be well in agreement but the *y*-velocity is predicted with large discrepancy compared with *x*- and *z*-velocity.

The comparisons suggest that although the numerical calculations can not substitute experimental work, especially for the case of complex flow such as in structured packing, the CFD simulation can play a role supplemental to experiment.

ACKNOWLEDGEMENTS

The authors wish to acknowledge the assistance by the staff in the State Key Laboratories of Chemical Engineering (Tianjin University).

NOMENCLATURE

d_h	hydraulic diameter [d_h＝4 (wetted area/wetted perimeter)], m
k	turbulent kinetic energy, $m^2 \cdot s^{-2}$
p	pressure, Pa
Δp	pressure drop, $Pa \cdot m^{-1}$
Re	Reynolds number for liquid phase ($Re = \rho u_s d_h / \mu$)
u_i	*i*-direction local velocity, $m \cdot s^{-1}$
u_s	superficial velocity, $m \cdot s^{-1}$
x, y, z	Cartesian coordinates, m

REFERENCES

1 Spiegel, L., Meier, W., "Distillation columns with structured packings in the next decade", *Trans IChemE*., **81**, 39—47 (2003).
2 Hodson, J.S., Fletcher, J.R., Porter K.E., "Fluid mechanical studies of structured distillation packings", In: Institution of Chemical Engineers Symposium Series, *AIChE*, New York, No.142, 999—1007(1997).
3 van Gulijk, C., "Using computational fluid dynamics to calculate transversal dispersion in a structured packed bed", *Comput*. *Chem*. *Eng*., **22**, S767—S770(1998).
4 Higler, A.P., Krishna, R., Ellenberger, J., Taylor, R., "Counter-current operation of a structured catalytically packed-bed reactor: Liquid phase mixing and mass transfer", *Chem*. *Eng*. *Sci*., **54**, 5145—5152(1999).
5 van Baten, J.M., Ellenberger, J., Krishna, R., "Radial and axial dispersion of the liquid phase within a KATAPAK-S structure: Experiments *vs*. CFD simulations", *Chem*. *Eng*. *Sci*., **56**, 813—821(2001).
6 van Baten, J.M., Krishna, R., "Gas and liquid phase mass transfer within KATAPAK-S structures studied using CFD simulations", *Chem*. *Eng*. *Sci*., **57**, 1531—1536(2002).
7 Petre, C.F., Larachi, F., Illiuta, I., Grandjean, B.P.A., "Pressure drop through structured packings: Breakdown into the contributing mechanisms by CFD modeling", *Chem*. *Eng*. *Sci*., **58**, 163—177(2003).
8 Larachi, F., Petre, C.F., Iliuta, I., Grandjean, B., "Tailoring the pressure drop of structured packings through

CFD simulations", *Chem. Eng. Process.*, **42**, 535—541(2003).

9 Zhang, P., Liu, C.J., Yuan, X.G., Yu, K.T., "CFD simulations of liquid phase flow in structured packed column", *J. Chem. Ind. Eng. (China)*, **55**(8), 1369—1373(2004).

10 Szulczewska, B., Zbicinski, I., Gorak, I., "Liquid flow on structured packing: CFD simulation and experimental study", *Chem. Eng. Technol.*, **26**(5), 580—584(2003).

11 Li, J., Huang, S.Y., Wang, X.M., "Numerical study of steam-water separators with wave-type vanes", *Chin. J. Chem. Eng.*, **15**(4), 492—498(2007).

12 Gu, F., Liu, C.J., Yuan, X.G., Yu K.T., "CFD simulation of liquid film flow on inclined plates", *Chem. Eng. Technol.*, **27**(10), 1099—1104(2004).

13 Raynal, L., Boyer, C., Ballaguet, J.P., "Liquid holdup and pressure drop determination in structured packing with CFD simulations", *Can. J. Chem. Eng.*, **82**, 871—879(2004).

14 Valluri, P., "Multiphase fluid dynamics in structured packings", Ph.D. Thesis, Imperial College London, University of London, UK.

15 Valluri, P., Matar, O.K., Hewitt, G.F., Mendes, M.A., "Thin film flow over structured packings at moderate Reynolds numbers", *Chem. Eng. Sci.*, **60**, 1965—1975(2005).

16 Armenante, P.M., Luo, C.G., Chou, C.C., Fort, I., Medek, J., "Velocity profiles in a closed, unbaffled vessel: Comparison between experimental LDV data and numerical CFD predictions", *Chem. Eng. Sci.*, **52**(20), 3483—3492(1997).

17 Li, M.Z., White, G., Wilkinson, D., "LDA measurements and CFD modeling of a stirred vessel with a retreat curve impeller", *Ind. Eng. Chem. Res.*, **43**, 6534—6547(2004).

18 Delnoij, E., Kuipers, J.A.M., van Swaaij, W.P.M., Westerweel, J., "Measurement of gas-liquid two-phase flow in bubble columns using ensemble correlation PIV", *Chem. Eng. Sci.*, **55**(17), 3385—3395(2000).

19 Sousa, R.G., Riethmuller, M.L., Pinto, A.M.F.R., Campos, J.B.L.M., "Flow around individual Taylor bubbles rising in stagnant CMC solutions: PIV measurements", *Chem. Eng. Sci.*, **60**(7), 1859—1873(2005).

20 Suekane, T., Yokouchi, Y., Hirai, S., "Inertial flow structures in a simple-packed bed of spheres", *AIChE J.*, **49**(1), 10—17(2003).

21 Gunjal, P.R., Ranade, V.V., Chaudhari, R.V., "Computational study of a single-phase flow in packed beds of spheres", *AIChE J.*, **51**(2), 365—378(2005).

22 Liu, G.Q., Ma, L.X., Liu, J., Material Properties Handbook in Chemistry and Chemical Engineering, 2nd edition, Chemical Industry Press, Beijing (2002).

23 Dantec Dynamics A/S, "BSA Flow Software (v2.1) Installation & User's Guide", P.O.Box 121, Denmark (2003).

24 User's Guide of Fluent 6.1, Fluent Inc., 2001.

25 Harris, C.K., Roekaerts, D., Rosendal, F.J.J., Buitendijk, F.G.J., Daskopoilos, Ph., Vreenegoor, A.J.N., Wang, H., "Computational fluid dynamics for chemical reactor engineering", *Chem. Eng. Sci.*, **51**, 1569—1594(1996).

26 Ng, K., Fentiman, N.J., Lee, K.C., Yianneskis, M., "Assessment of sliding mesh CFD predictions and LDA measurements of the flow in a tank stirred by a Rushton impeller", *Trans. IChemE*, **76**, 737—747(1998).

27 Li, M.Z., White, G., Wilkinson, D., "LDA measurements and CFD modeling of a stirred vessel with a retreat curve impeller", *Ind. Eng. Chem. Res.*, **43**, 6534—6547(2004).